Fluid Quantification and Kerogen Assessment in Shales Using ^{13}C and ^{1}H Magnetic Resonance Measurements

Mohammad Sadegh Zamiri[1], *Naser* Ansaribaranghar[1,2], *Andrés* Ramírez Aguilera[1], *Florea* Marica[1], and *Bruce J.* Balcom[1,*]

[1]UNB MRI Research Centre, Physics Department, University of New Brunswick, Fredericton, NB E3B 5A3, Canada
[2]Department of Chemical Engineering, University of New Brunswick, Fredericton, NB E3B 5A3, Canada

Abstract. A vast amount of hydrocarbon can be found in shale formations around the world. Hydrocarbon production from these formations is expected to contribute significantly to future energy supplies. For economic hydrocarbon production, it is essential to identify shale formation sectors with reservoir quality. A sector with reservoir quality contains a substantial amount of hydrocarbon and organic matter known as kerogen. Moreover, the class of kerogen is indicative of the type and quality of hydrocarbons present. Kerogen classification is performed using Van Krevelen diagrams which are a plot of H/C and O/C ratios. Routine core analysis techniques for fluid quantification and kerogen assessment in shales are sample destructive, time-consuming, and prone to errors. Magnetic resonance (MR) methods are increasingly utilized for shale characterization due to their ability to provide a wide range of parameters that offer insights into the petrophysics and geochemistry of shale samples. So far, MR methods for shale characterization have focused on probing hydrogen that resides in various shale components such as brine, oil, kerogen, and minerals. Various source of ^{1}H in shales results in multicomponent MR signal, making it challenging to distinguish between various shale components. In this work, naturally occurring ^{13}C was probed for shale characterization. Among shale species, only kerogen and oil yield detectable ^{13}C MR signal. A mature and an immature oil-rich shale samples were used in this study. The ^{13}C MR signal was resolved and quantified for kerogen and oil using 2D MR relaxation correlation measurement. Furthermore, we determine the H/C ratio which is an indication of kerogen class, incorporating ^{13}C and ^{1}H MR measurements.

1 Introduction

Shale formations hold significant amounts of hydrocarbon reserves globally [1]. With ever-rising energy demand, the prospects of growth in production from these formations are also high [2]. Shale formations are traditionally viewed as the source rock for conventional hydrocarbon reservoirs [3]. They contain kerogen, a complex semi-solid organic matter that when exposed to elevated temperatures as a result of geological burial, it produces hydrocarbons [1,4]. Furthermore, shale formations are viewed as the cap rock for conventional reservoirs due to their tight and impermeable nature. Therefore, they generally lack reservoir quality [1]. Recent technological advancements, namely hydraulic fracturing and horizontal well drilling has made production from these formations more viable. Despite these advancements, the key to economic hydrocarbon production from shales lies in identifying sectors within these formations that offer the highest reservoir quality. This critical task involves accurate shale characterization [1,3].

Some of the important factors in shale characterization include estimation of hydrocarbon content, kerogen quality, and kerogen class [1,3]. Conventional methods to measure hydrocarbon content in shales involve extraction of fluids. Methods such as Dean Stark and retort are conventionally used for this purpose [5,6]. Kerogen classification involves the Van Krevelen diagram, which is a plot of H/C and O/C. There are four kerogen classes based on the Van Krevelen diagram. A high H/C content can result from high-quality kerogen, typically class I or II, or indicate immature kerogen. RockEval analysis is used as an analogous measurement to elemental analysis of kerogen to give estimation of H/C and O/C. During RockEval analysis, the shale sample is heated in an inert environment. The gases and fluids entrained in the flowing stream over the shale sample are analyzed to give an estimation of H/C and O/C [7,8]. These traditional core analysis techniques for quantifying fluids and assessing kerogen in shale formations involve physically extracting and processing samples, which not only destroys the samples but also is time-consuming and susceptible to errors [5,6]. As a result, there is a growing need for alternative methods that can provide more efficient and accurate assessments of fluid content and kerogen properties in shale formations.

Alternately, magnetic resonance (MR) methods are fast and non-destructive. Commonly, ^{1}H MR signal is used for shale characterization [9-16]. The shale ^{1}H MR

* Corresponding author: bjb@unb.ca

signal poses some challenges. (1) signal is short-lived. This makes signal detection and quantification difficult. (2) shale MR signal is multi component. This is because shale ^{1}H MR signal originates from various shale species, namely, water, oil, and kerogen. Therefore, the MR signal should be first resolved for its species [17,18]. Despite developments in MR methods tailored to shale samples, the challenge to unambiguously and quantitatively separate shale MR signal components still remains.

In this work, naturally occurring ^{13}C is measured in shale samples. Among shale species, only kerogen and oil produce a detectable ^{13}C MR signal. [19,20]. Therefore, there are fewer shale species contributing to the MR signal. This makes signal differentiation and quantification easier. Furthermore, ^{13}C signal lifetimes are longer than that from ^{1}H measurements, allowing for a more quantitative signal detection. The ^{13}C MR signal is resolved for kerogen and oil using 2D MR relaxation correlation measurement. The ^{1}H MR signal is compared to that of ^{13}C measurement. Furthermore, we determine H/C ratio, which is an indication of kerogen class, incorporating ^{13}C and ^{1}H MR measurements for a mature and immature shale sample.

2 Theory

The relaxation of hydrocarbons due to dipole-dipole interactions can be described by Bloembergen-Purcell-Pound (BPP) theory, given in Eqs. 1 and 2 [7,21,22].

$$\frac{1}{T_1} = \left(\frac{\mu_0}{4\pi}\right)\gamma^4\hbar^2 I(I+1)\frac{1}{5r^6}[J(\omega) + 4J(2\omega)] \quad (1)$$

$$\frac{1}{T_2} = \left(\frac{\mu_0}{4\pi}\right)\gamma^4\hbar^2 I(I+1)\frac{1}{5r^6}[3J(0) + 4J(\omega) + 2J(2\omega)] \quad (2)$$

where I is the spin number and equals $1/2$ for both ^{1}H and ^{13}C, μ_0 is the vacuum permeability, $\hbar$ is Planck's constant divided by $2\,\pi$ and r is the distance between neighboring diploes. γ is the gyromagnetic ratio, and is 42.57 and 10.71 MHz/T for ^{1}H and ^{13}C, respectively. The spectral densities, $J(\omega)$ which are the Fourier transform of the autocorrelation functions of local magnetic field fluctuations are in the form of Lorentzian function. $J(\omega)$ are functions of frequency and correlation time, τ_c which characters molecular motion. In the case of low frequency and rapid motion (short correlation time), $\omega\tau_c \leq 1$ and ratio T_1/T_2 approaches one. In contrast, for solid-like materials molecular motion is slow, and $\omega\tau_c \geq 1$ and T_1/T_2 exceeds unity.

Oil species may also contain asphaltene molecules which contain free radicals. Consequently, an alternative relaxation mechanism of hydrocarbon material is additional paramagnetic interactions with free radicals in the asphaltene molecules that can shorten the relaxation lifetimes [23].

As given by Eqs. 1 and 2, the possible relaxation mechanisms originally developed and experimentally tested for ^{1}H-^{1}H interactions were discussed in [22]. However, in this study, we investigate ^{13}C relaxation as well. Given that both ^{1}H and ^{13}C nuclei are spin 1/2 particles, we hypothesize that ^{13}C relaxation will be analogous to that of ^{1}H.

3 Experimental and Methods

3.1 Shale Rocks

Two shale samples designated as sample E10 and sample H2 were used in this study. Sample E10, from the Eagle Ford Formation, is an outcrop sample with dimensions of 1.5 inches in diameter and 2 inches in length. This sample was used in its original, as-received condition for all measurements. Sample H2, on the other hand, is a mature shale sample with dimensions of 1 inch in diameter and 1.5 inches in length. This sample was saturated with water prior to testing.

3.2 MR Instrumentation

MR measurements were acquired using a cryogen free variable field superconducting magnet (MR Solutions, Guildford, Surrey, UK). ^{13}C and ^{1}H measurements were acquired at a resonance frequency of 33.7 MHz, which corresponds to a magnetic field of 0.79 T for ^{1}H and 3 T for ^{13}C. The RF probe was a homemade birdcage. The magnet was permanently connected to a magnet power supply (Cryomagnetics, Inc., TN, US). GIT systems software (Green Imaging Technologies, Inc., NB, Canada) was employed to execute MR measurements.

3.3 MR Measurements

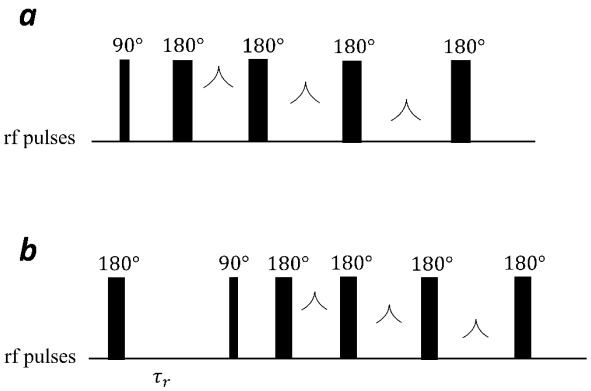

Fig. 1. (a) CPMG measurement modified with a variable echo time to facilitate detection of short T_2 components. (b) 2D T_1-T_2 relaxation correlation measurement, consists of two parts: a T_1 recovery part with a variable time τ_r, and a detection part, similar to Figure 1a.

A modified CPMG (Carr-Purcell-Meiboom-Gill) pulse train with variable echo time, Figure 1a, was used to acquire T_2 distribution of shale samples for both ^{13}C and ^{1}H measurements. 2D T_1-T_2 relaxation correlation measurements were performed according to the pulse sequence shown in Figure 1b. The pulse sequence consists

of two main parts: a T_1 recovery part and an acquisition part. In the T_1 recovery stage, the longitudinal magnetization was inverted using a 180-degree pulse, followed by partial recovery over the variable time interval τ_r. In the acquisition part, the signal was recorded using the modified CPMG method, which collected the data with a variable echo time spacing. The pulse sequence shown in Figure 1b was repeated with various τ_r values that were logarithmically spaced to cover the T_1 recovery of the sample.

The MR acquisition parameters for the ^{1}H and ^{13}C measurements were as follow: The 90-degree pulse duration was 10 and 40 μs for ^{1}H and ^{13}C, respectively. 512 echoes were acquired with echo times that were varied, during the CPMG echo train, with consecutive differences increasing logarithmically from 164 μs to 4 s. Five time-domain data points were acquired at each echo time with a dwell time of 5 μs. 32 and 128 signal averages were performed for ^{1}H and ^{13}C, respectively. The total measurement time of 11 mins for ^{1}H yielded a typical signal-to-noise ratio (SNR) of 1000, a 43-minute measurement for ^{13}C produced an SNR of 35.

For T_1-T_2 measurements, in the T_1 recovery part, τ_r varies logarithmically from 60 μs to 11.5 s with 60 and 15 τ_r values for ^{1}H and ^{13}C, respectively. The parameters for acquisition part of the 2D T_1-T_2 was similar to that of CPMG measurement. 8 and 128 signal averages were performed for ^{1}H and ^{13}C, respectively. The total measurement time of 1.5-hour for ^{1}H yielded a typical SNR of 35, a 10-hour measurement for ^{13}C resulted in an SNR of 527.

3.4 Data Processing

Signal, $S(\tau_r, t)$ in the T_1-T_2 measurement can be described by a Fredholm integral of the first kind, shown in Eq. 3 [23].

$$S(\tau_r, t) = \iint \left(1 - \exp\left(-\frac{\tau_r}{T_1}\right)\right) \exp\left(-\frac{t}{T_2}\right) \mathcal{F}(T_1, T_2) dT_1 dT_2 \quad (3)$$

The joint probability distribution, $\mathcal{F}(T_1, T_2)$ is the resolved signal in the 2D T_1-T_2 relaxation correlation map, with ^{1}H signal from ^{1}H-bearing species such as oil, water, and kerogen, and ^{13}C signal from ^{13}C-bearing species such as oil and kerogen in the shale sample. The relaxation decay of magnetization exhibited predominantly exponential behavior in the samples analyzed in this study. Therefore, exponential functions were employed in Eq. 3 to characterize the signal.

A Fast Laplace Inversion algorithm (Laplace Inversion Software, Schlumberger-Doll Research) written in the MATLAB environment (MathWorks, Natick, MA) was used to produce 2D T_1-T_2 relaxation correlation maps according to Eq. 3.

4 Result and Discussions

4.1 CPMG Measurements

Figure 2a depicts the ^{13}C T_2 measurements from E10 and H2 shale samples. Absence of ^{13}C in the brine means that hydrocarbon species, oil and kerogen solely yield the ^{13}C signal. The semi-solid shale species, kerogen yields the short T_2 component with ^{13}C T_2 of ~ 0.4 ms. In Figure 2b, the ^{1}H T_2 distribution from E10 and H2 shale samples are shown. Kerogen shows a ^{1}H T_2 of ~0.1 ms. It is important to note that due to limitations in the instrument's echo time, the short ^{1}H T_2 component may not have been fully resolved. Therefore, the kerogen signal peak may be shifted to the longer T_2 values. Figure 2 demonstrates that the T_2 lifetime of the kerogen signal component, as measured by ^{13}C, is longer than that measured by ^{1}H. Consequently, the effect of echo time limitation on the T_2 signal component in ^{13}C measurements is reduced.

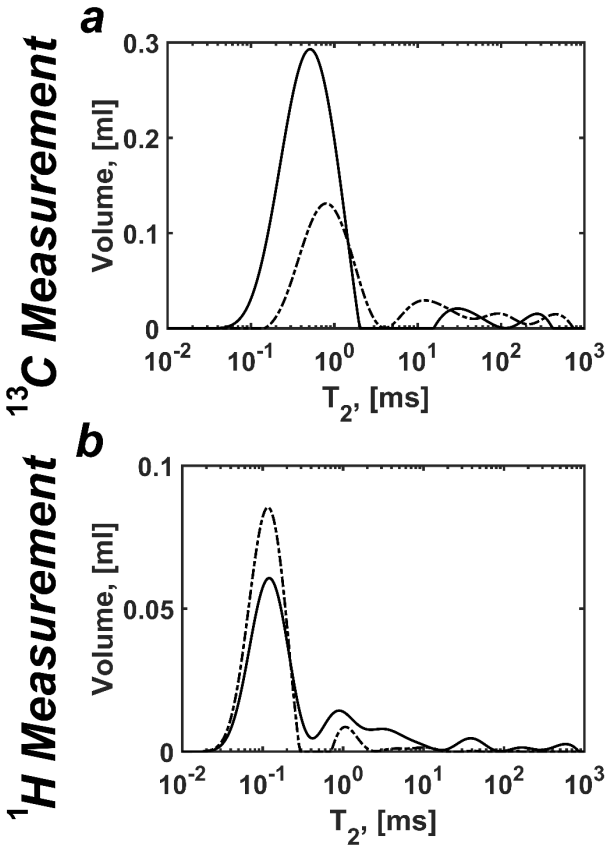

Fig. 2. (a) ^{13}C T_2 distribution for sample E10 (dashed line) and sample H2 (solid line). Water signal is absent in ^{13}C measurement. The short T_2 component is kerogen, the long T_2 components are oil species in shales. (b) ^{1}H T_2 distribution for sample E10 (dashed line) and sample H2 (solid line). Water signal overlaps with that of kerogen and oil. Sample H2 was saturated with water. Therefore, the oil signal was largely masked by that of water. T_2 of kerogen from ^{13}C is longer than that from ^{1}H.

The longer T_2 components in Figure 2 are associated with the shale oil species. Water signal is present in ^{1}H T_2 distribution measurement shown in Figure 2b. The water signal component can overlap with that of oil and kerogen. Due to this signal overlap, it is not possible to differentiate for kerogen, oil, and water species using 1D relaxation measurement for these shale samples. Figure 2 demonstrates that, unlike ^{1}H CPMG measurements, a simple ^{13}C CPMG is sufficient to discriminate and

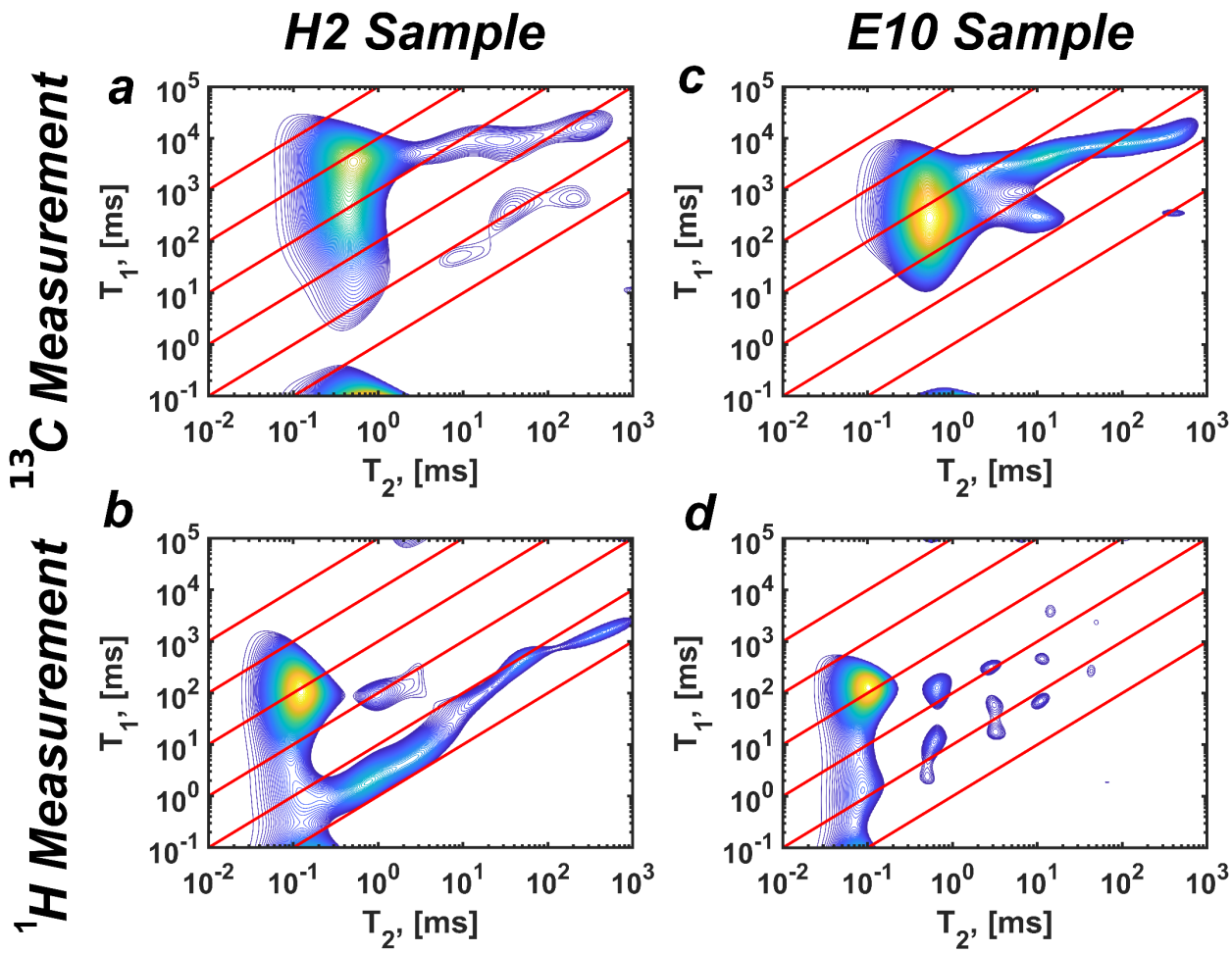

Fig. 3. 2D T_1-T_2 relaxation correlation measurement of (a) H2 sample using ^{13}C, (b) E10 sample using ^{13}C, (c) H2 sample using ^{1}H, and (d) E10 sample using ^{1}H. Water signal is absent in the ^{13}C measurements. The short T_2 relaxation signal peak is associated with kerogen. Long T_1 and T_2 signal components belong to oil species. Water in ^{1}H measurements shows short T_1 and T_2 signal peaks. Red diagonal lines are T_1/T_2 = 1, 10, 10^2, 10^3, 10^4, 10^5, 10^6.

quantify the kerogen and oil shale species. Figure 2 also shows the absence of a water signal in the ^{13}C spectrum, clearly observable in sample H2. This sample was saturated with water, as indicated by the large signal intensity with a long T_2 in the ^{1}H spectrum. In contrast, the ^{13}C spectrum display a smaller signal intensity with a long T_2, because of the absence of water signal component.

The signal amplitude from the ^{13}C CPMG measurements in Figure 2 were calibrated to determine volume of oil and carbon content of kerogen. The reference sample used for calibration was decane with known volume. The integrated signal intensity of the kerogen and oil signal peaks in the T_2 distribution gives the quantity of the corresponding shale species for the E10 and H2 shale samples. Kerogen contained 0.24 and 0.6 mole C for sample E10 and H2, respectively, assuming natural ^{13}C abundance of 1.1%. Oil content was measured to be 1.65 and 0.77 ml for sample E10 and H2, respectively. Signal calibration for kerogen was performed to convert signal intensity to content in moles, whereas for oil species, it was converted to volume. This distinction was made because oil content is usually reported in volume, while for kerogen, the goal is to quantify the H/C ratio, as discussed in the next section.

An important consideration in measuring carbon content in the shale samples using ^{13}C MR measurements is the assumption that ^{13}C density in shale samples is similar to that in the reference sample, which was decane in this study. A preliminary study shows that ^{13}C density variation from various oil samples around the world do not significantly affect volumetric quantification of phases [25]. However, variation of ^{13}C density among kerogen samples has not been tested. To convert signal intensity to moles for kerogen, it was assumed that the signal intensity per mole is the same for kerogen and the reference sample.

4.2 2D T_1-T_2 Measurements

Figure 3 shows the 2D T_1-T_2 measurements from ^{1}H and ^{13}C for both E10 and H2 shale samples. The ^{13}C measurements lack water signal, therefore, there are fewer signal components present in the ^{13}C MR response. This reduction in signal overlap enhances the quantitative determination of MR properties using ^{13}C compared to ^{1}H MR measurements of shales. This leads to a better fluid differentiation and quantification.

According to Eqs. 1 and 2, kerogen, a semi-solid material shows a high T_1/T_2 signal component in both ^{1}H

and ^{13}C T_1-T_2 correlation maps. In Fig. 3, T_1/T_2 ratios for kerogen in sample E10 from ^{13}C and ^{1}H measurements were 711 and 920, respectively, and those for sample H2 were 1870 and 790. This is due to slow molecular motions in solids. In Eqs. 1 and 2, $J(\omega)$ does not change between ^{1}H and ^{13}C measurements since both are performed at the same frequency, 33 MHz. However, the gyromagnetic ratio of ^{13}C is one fourth that of ^{1}H. According to Eq. 1, assuming similar dipole-dipole distance for ^{1}H and ^{13}C, T_1 should increase by a factor of 256 for ^{13}C compared to ^{1}H. In Figure 3, although T_1 for kerogen increased by a factor of 4 and 9 between ^{13}C and ^{1}H measurements for samples E10 and H2, respectively, this increase was not according to Eq. 1. This suggests that relaxation due to interactions with paramagnetics may be occurring in addition to dipole interactions, as discussed in the Theory section. Oil species in shale samples show a lower T_1/T_2 ratio compared to that of kerogen. Oil T_1/T_2 ratio for sample E10 was 140 and 36 for ^{13}C and ^{1}H measurements, respectively. Oil T_1/T_2 ratio for sample H2 was 145 and 10 for ^{13}C and ^{1}H measurements, respectively. Comparing kerogen and oil signal components in Figure 3 from ^{1}H and ^{13}C measurements, similar ^{1}H and ^{13}C relaxation behavior is observed, given that they are both spin ½ nuclei.

Water signal, only visible in the ^{1}H correlation map, shows a low T_1/T_2 signal characteristic, originating from high surface relaxation of water in small pores. T_1/T_2 ratio of water signal peak for sample H2 and E10 was 2.5 and 20, respectively. Tables 1 and 2 summarize the ^{1}H and ^{13}C relaxation times of shale species.

Table 1. ^{1}H and ^{13}C log-mean relaxation times of various shale species for H2 sample.

Sample	H2			
Nucleus	^{13}C measurements		^{1}H measurements	
Lifetime	T_{1LM}	T_{2LM}	T_{1LM}	T_{2LM}
Kerogen	748 ms	400 µs	79 ms	100 µs
Oil	4.1 s	28.2 ms	250 ms	24.7 ms
Water	–	–	3 ms	1.2 ms

Table 2. ^{1}H and ^{13}C log-mean relaxation times of various shale species for E10 sample.

Sample	E10			
Nucleus	^{13}C measurements		^{1}H measurements	
Lifetime	T_{1LM}	T_{2LM}	T_{1LM}	T_{2LM}
Kerogen	370 ms	520 µs	92	100 µs
Oil	3.2 s	22.9 ms	65 ms	1.8 ms
Water	–	–	1.7 ms	84 µs

4.3 Kerogen Assessment

The signal intensity from ^{1}H and ^{13}C measurements in Figure 3 are calibrated using a decane sample with a known volume. Table 3 summarizes the ^{1}H and ^{13}C content of shale species.

Van Krevelen diagram which is a plot of H/C versus O/C is commonly used to classify kerogen in shale samples (I, II, III, and IV). The ratio H/C in kerogen is vital for determining kerogen class, and maturity level. The kerogen class from I to IV contain progressively lower amounts of H/C, and are a lower quality kerogen. Furthermore, as kerogen undergoes petroleum generation, the chemical changes result in a mobile phase rich in hydrogen and a carbon rich residue. This reaction causes systematic changes in kerogen (geothermal maturity), leading to a decrease in H/C ratio. Combining ^{1}H and ^{13}C measurements, one can quantify H/C ratio, which is a valuable tool for the geochemical assessment of kerogen in shale formations.

Table 3. ^{1}H and ^{13}C content of shale species.

Species	^{1}H measurements		^{13}C measurements	
Sample	H2	E10	H2	E10
Kerogen	0.16 mol H	0.2 mol H	0.4 mol C	0.18 mol C
Oil	0.56 ml	0.64 ml	0.81 ml	1.14 ml
Water	1.13 ml	0.36 ml	–	–

Using the ^{1}H and ^{13}C molar values reported in Table 3 for the kerogen peak, one can obtain molar H/C ratios for the shale samples. Figure 4 shows the H/C of 1.1 and 0.4 for samples E10 and H2, respectively on the Van Krevelen diagram. Sample E10, taken from an outcrop, contains either a partially matured kerogen of class I or II, while the H2 sample contains mature kerogen, as indicated by its low H/C ratio. The kerogen class for sample H2 cannot be determined since its H/C ratio lies at the intersection of the kerogen class curves. Additional information on the O/C ratio may help classify the kerogen type for this sample.

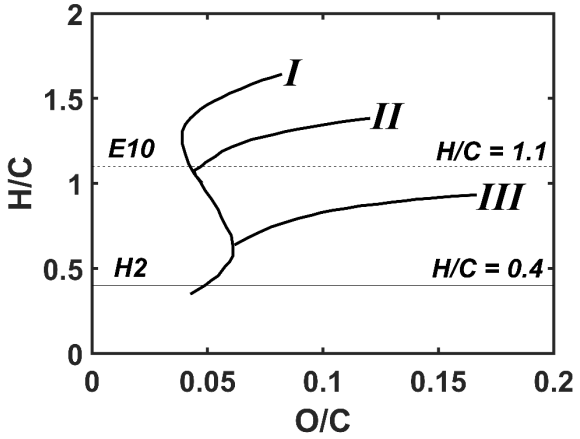

Fig. 4. Van Krevelen diagram of molar H/C ratio against molar O/C ratio showing different kerogen classes. The dashed line corresponds to H/C for sample E10, and the solid horizontal line is H/C for sample H2. Shale sample H2 contains mature kerogen, and sample E10 is a partially mature kerogen of either class I or II.

In this study, we have demonstrated the direct measurement of ^{1}H and ^{13}C to determine the H/C ratios. However, the lack of oxygen measurement results in an incomplete characterization, as the horizontal axis of the Van Krevelen diagram remains unexplored. To address this limitation, future studies could consider employing MR measurements of ^{17}O to quantify oxygen in shales. It is noteworthy that ^{17}O and ^{13}C exhibit a relative sensitivity of 1.1×10^{-5} and 1.8×10^{-4} respectively, compared to ^{1}H. The results presented in this paper could benefit from

companion conventional measurements of carbon content in kerogen. Comparing the H/C ratios measured using the described method with conventional measurements can help establish this technique as a standard practice for kerogen classification.

5 Conclusion

In ^{1}H MR measurements of shale, the water signal commonly overlaps with that of kerogen and oil in a simple CPMG measurement. Therefore, 2D relaxation correlation measurements are required to differentiate signal components. In this paper, ^{13}C measurements are employed to resolve and quantify shale signal, and perform kerogen assessment. ^{13}C MR signal is solely from hydrocarbon species, oil and kerogen. We tested a mature and an immature shale sample. Oil and kerogen signal components were resolved in the ^{13}C T_2 distribution and 2D T_1-T_2 relaxation correlation measurements. The signal intensity was then calibrated to give carbon content of kerogen and oil quantity. It was shown that a simple ^{13}C CPMG measurement is sufficient to distinguish oil and kerogen signal components. ^{13}C measurements were combined with ^{1}H measurements to give H/C for the kerogen in the two shale samples. The level of maturity and quality of kerogen were determined for the shale samples.

Authors thank the Canada Chairs program for a Research Chair in Material Science MRI [950-230894].

References

1. R. Rezaee, *Fundamentals of gas shale reservoirs*, (Hoboken, Wiley, 2015).
2. Annual Energy Outlook, https://www.eia.gov/outlooks/aeo/pdf/AEO2023_Narrative.pdf (2023).
3. Y.Z. Ma, S.A. Holditch, *Unconventional oil and gas resources handbook*, (Elsevier, 2016).
4. R.M. Garrels, F.T. Mackenzie, Science **163**, 570-571, (1969).
5. C. McPhee, J. Reed, I. Zubizarreta, *Core Analysis: A Best Practice Guide* (Elsevier, Amsterdam, 2015).
6. API. *Recommended practices for core analysis*, (Washington, American Petroleum Institute, 1998).
7. M.H. Engel, S.A. Macko, *Organic geochemistry: principles and applications* (Boston, MA, Springer, 1993).
8. B. Tissot, B. Durand, J. Espitalie, A. Combaz, AAPG Bull **58**(4), 809 (1974).
9. M. Fleury, M. Romero-Sarmiento, Characterization of shales using T_1–T_2 NMR maps. J Petrol Sci Eng. **137**, 55–62 (2016).
10. Y.Q. Song, R. Kausik, Prog Nucl Mag Res Sp. **112–113**, 17–33 (2019).
11. D. Yang, R. Kausik, Energ Fuel **30**(6), 4509–4519 (2016).
12. R. Kausik, K. Viswanathan, C. Cao Minh, L. Zielinski, B. Vissapragada, R. Akkurt, Y.Q. Song, C. Liu, S. Jones, E. Blair, *SPE Annual Technical Conference and Exhibition*, SPE-147198-MS (2011).
13. R. Kausik, K. Fellah, L. Feng, G. Simpson, Petrophysics **58**(4), 341–351 (2017).
14. M.S. Zamiri, B. MacMillan, F. Marica, J. Guo, L. Romero-Zerón, B.J. Balcom, Fuel **284**, 119014 (2021).
15. M.S. Zamiri, F. Marica, L. Romero-Zerón, B.J. Balcom. Che Eng J. 428, 131042 (2022).
16. Y. Liu, X. Wang, G.J. Hirasaki, E.G. Vinegar, H.J. Vinegar, P.M. Singer, Fuel 333, 126223 (2023).
17. M.S. Zamiri, J. Guo, F. Marica, L. Romero-Zerón, B.J. Balcom, *International Symposium of the Society of Core Analysts*, SCA2022-013 (2022).
18. M.S. Zamiri, J. Guo, F. Marica, L. Romero-Zerón, B.J. Balcom, Petrophysics **64**(3), 384-401 (2023).
19. N. Ansaribaranghar, M.S. Zamiri, L. Romero-Zerón, F. Marica, A. Ramírez Aguilera, D. Green, B. Nicot, B.J. Balcom, International *Symposium of the Society of Core Analysts*, SCA2023-018, (2023).
20. N. Ansaribaranghar, M.S. Zamiri, L. Romero-Zerón, F. Marica, A. Ramírez Aguilera, D. Green, B. Nicot, B.J. Balcom, *International Symposium of the Society of Core Analysts*, SCA2023-005, (2023).
21. N. Bloembergen, E. Purcell, R. Pound, Phys Rev. **73**(7), 679–712 (1948).
22. P. Singer, A.V. Parambathu, X. Wang, D. Asthagiri, W. Chapman, G.J. Hirasaki, J Phys Chem B **124**, 4222–4233 (2020).
23. S. Stapf, A. Ordikhani-Seyedlar, N. Ryan, C. Mattea, R. Kausik, D. Freed, Energ Fuel, **28**(4), 2395–2401 (2014).
24. Y.Q. Song, L. Venkataramanan, M.D. Hürlimann, M. Flaum, P. Frulla, C. Straley, J. Magn. Reson. **154**, 261–268 (2002).
25. N. Ansaribaranghar, M.S. Zamiri, L. Romero-Zerón, F. Marica, A. Ramírez Aguilera, M.J. Dick, D. Green, B. Nicot, B.J. Balcom, *International Symposium of the Society of Core Analysts*, SCA2024, (2024).